Simulation of Heat Transfer during Artificial Ground Freezing Combined with Groundwater Flow

Rui Hu[*1], Quan Liu[1]

[1] School of Earth Science and Engineering, Hohai University, Nanjing, China
*Corresponding author: No.8 Fochengxi Road, Nanjing, China, rhu@hhu.edu.cn

Abstract: Based on the heat transfer and seepage theory in porous media with finite element method, a 2D numerical model was established to simulate the changes of temperature field and the process of freezing wall formation during a strengthening project of a metro tunnel with artificial ground freezing method (AGF). The simulation results show that the freezing wall appears in an asymmetrical shape as the horizontal groundwater flow is normal to the axial of the tunnel. Along the groundwater flow direction, freezing wall forms slowly and on the upstream side the thickness of the freezing wall is thinner than that on the downstream side. The closure time of the freezing wall increases at the middle of the both up and downstream sides. The average thickness of the freezing wall on the upstream side is mostly affected by the groundwater flow velocity.

Keywords: Artificial ground freezing method, groundwater flow, temperature field, freezing wall, effective hydraulic conductivity.

1. Introduction

The artificial ground freezing (AGF) method has been widely used in civil and mining engineering. Its principle is to circulate a fluid refrigerant (ca. -30°C) through a pre-buried pipe network in the subsurface in order to form a freezing wall for construction strengthening. The knowledge of the in-situ temperature distribution is the key factor with respect to the development of the freezing wall. The main physical process is a transient heat conduction phenomenon with phase change. In common cases, the temperature change is only considered as a heat conduction process. However, with groundwater of high flow velocities, the influence of the water-ice phase change on the flow properties should not be neglected. In this work, we performed a case study of a strengthening project of a metro tunnel with AGF method, considering the influence of groundwater flow.

Artificial ground freezing method (AGF), patented by Poetch in Germany in 1883, is a construction technology which freezes the water in the ground by artificial refrigerant to create a high-strength freezing wall. In this study, the AGF method is applied to simulate a soil body strengthening project at the portal of a metro tunnel in Guangzhou, China. The location of the project is shown in **Figure 1**. With this method, the circulation of refrigerant (-30°C brine) in the pre-buried pipes can reduce the subsurface temperature till the pore water freezes and the freezing wall forms. Hence, the temperature distribution in the underground is the key controlling factor during the artificial freezing activities.

Figure 1. The location of the project in Guangzhou, China. (Note that the point A indicates the overview position on the ground. The real project position is below this point in the subway underground)

2. Model Definition

In this project, within the freezing area, the formation is muddy sand. The groundwater flow direction is mainly horizontal and normal to the axial of tunnel. Thus, we used a 2D model to simplify the simulation of heat transport in a saturated aquifer. The model geometry is shown in **Figure 2a**. Both of the length and height of this model are 20m. Five monitoring points are set to verify the accuracy of this numerical model by the comparison of transient temperature value between the in-situ measurements and the calculated results. **Figure 2b** is the model grid meshed by COMSOL Multiphysics®.
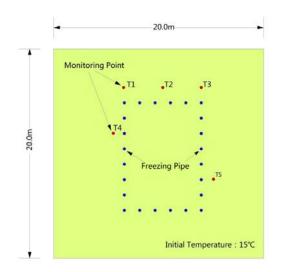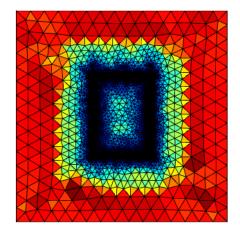
Figure 2a. Model geometry

Figure 2b. **Model** grid (meshing by COMSOL)

2.1 Model Assumptions

This model is simplified to an ideal case with the following assumptions:

(1) The ice is immobile, the medium is non-deformable;
(2) The aquifer is fully saturated and its total porosity remains constant;
(3) The freezing point depression due to solute concentrations is negligible.

2.2 Governing Equations

In a saturated aquifer, the heat transport process mainly includes the release of latent heat, heat conduction and heat convection. The temperature field T is governed by the heat transport equation:

$$C_{eq}\frac{\partial T}{\partial t} - \nabla[\lambda_{eq}\nabla T] + C_f \bar{u}\nabla T - \rho_w L\frac{\partial S_w}{\partial T} = Q_G \qquad (1)$$

where λ_{eq} is bulk thermal conductivity (calculated by volumetric average approximation); $\bar{u}$ is seepage velocity, calculated by the Darcy's law; S_w is the saturation of water in the pores; $-\partial S_w / \partial T$ is solid fraction, which is equal to the derivative of S_w with respect to T.

The distribution of temperature in the aquifer has a great influence on seepage field in this case. On the one hand, because of ice formation during the phase change, the original pore channel is blocked which may temporarily change the groundwater flow systems. On the other hand, although ice formation is accompanied by the expansion of volume, the pore water, at that moment, has much lower flow ability in frozen area. Therefore, the water flow in the frozen zone can be ignored with respect to the effect of pore expansion. The total ground water flow field is governed by the Darcy's law as followed:

$$(1 - \varepsilon S_i)S_{OP}\frac{\partial p}{\partial t} + \nabla[-\frac{k_r K\rho}{\mu} \cdot (\nabla p + \rho_w g\nabla D)]$$

$$= Q_S + \varepsilon(\rho_w - \rho_i)\frac{\partial S_i}{\partial t} \qquad (2)$$

, where S_{OP} is the specified pressure storativity and k_r is the relative permeability (used to represent the decrease of permeability in the water-ice phase transformation zone), described by Heaviside function.

2.3 Initial & Boundary Conditions

Temperature: according to the prior in-situ temperature monitoring data at destination freezing depth, the initial ground temperature is about 15°C. The box chart of initial temperatures in different thermo-observation holes is shown in **Figure 3a**.

Temperature boundary condition: the lateral wall of freezing pipe is the cooling source of freezing system and the change of lateral wall temperature has a great effect on temperature distribution in the whole system. The temperature monitoring values of main-pipe, through which the refrigerant can flow to the freezing wall, can be approximately used to estimate the lateral wall temperature. According to the temperature monitoring data of loop main-pipe (T_{out}) during monitoring period (40 days), the lateral wall temperature fitting function and curve are shown in **Figure 3b**.
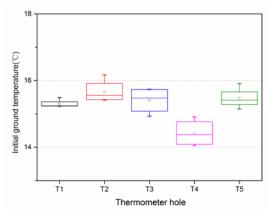

Figure 3a. Box chart of initial ground temperature
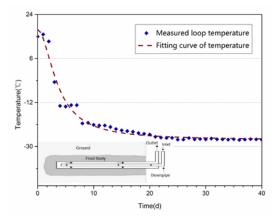

Figure 3b. Fitting curve of pipe wall temperature (T_{out})

Groundwater flow: the flow velocity obtained through field test is 0.2m/d. Based on the Darcy's law, the head difference between up and downstream is calculated as 0.8m.
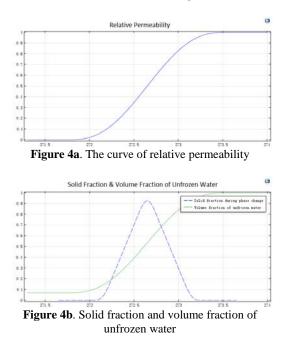
3. Use of COMSOL Multiphysics® Software

With the simulation software COMSOL Multiphysics®, a 2D cross section of a horizontal AGF project (**Figure 2a**) is selected and a numerical model is set up, which is based on full coupling of temperature and flow fields by combining physical interfaces of Darcy's Law and Heat Transfer in Porous Media. Firstly, the Darcy's velocity $\bar{u}$ is selected as a coupling variable and linked to the temperature field. Subsequently, as the pore water gradually turns into ice, the permeability in freezing zone is decreased. At this phase, we introduce a variable of effective hydraulic conductivity k_r which can be described by a function of temperature change. At this point, k_r is assigned by a step function (**Figure 4a**):

$$k_r(T) = (1 - k_{rw}) flc2hs(T - T_P, \delta T) + k_{rw} \qquad (1.3)$$

where $flc2hs$ is a Heaviside function and k_{rw} is an arbitrary small minimum value for frozen area permeability (cannot be equal to zero, or the flow equation cannot be solved. Here it is limited at 10^{-6}.)
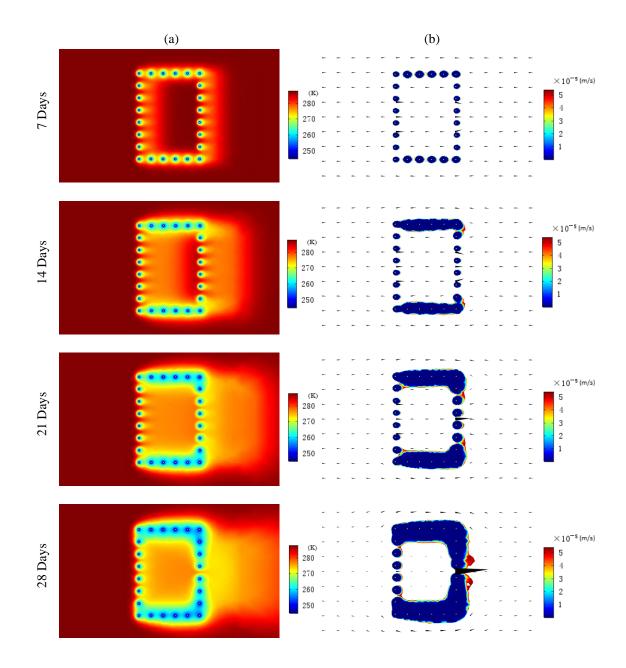
Similarly, the saturation of water S_w and its derivative curves are shown in **Figure 4b**.

Figure 4a. The curve of relative permeability

Figure 4b. Solid fraction and volume fraction of unfrozen water

The energy conservation problem during freezing phase change is solved by apparent heat capacity method and the related parameter change is described by a step function (**References 2**). The corresponding mesh is generated through automatic remeshing (**Figure 2b**). This model is validated with in-situ temperature observations.

4. Results and Discussion

Table 1 in the Appendix shows the parameters used for the calculation in this model. The simulation results of temperature and permeability coefficient at various times (7d, 14d, 21d, 28d, and 35d) are shown in **Figure 5**.
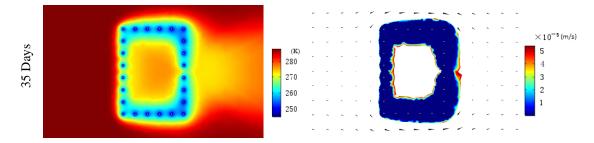
Figure 5. (a)Temperature distribution and (b) permeability coefficient (temperature below 0°C) results & Darcy's velocity field (black arrows) for project example at various times

The temperature distribution maps (**Figure 5a**) show that as the freezing time increases, the cold temperature from freezing pipes is mainly conducted to downstream and has less impact on upstream. The permeability coefficient chart (**Figure 5b**) implies the formation process of freezing wall. The freezing walls at the top and bottom form faster than that at the up-downstream. On the 35th day (closure time), the freezing wall was completely closed.
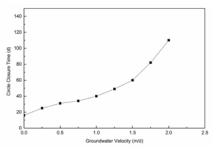

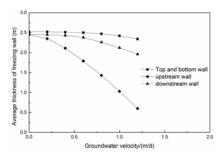**Figure 6**. Relationship between freezing wall circle closure time and flow velocity

Figure 7. Relationship between average wall thickness in each direction and corresponding flow velocity

Figure 6 shows the variation curve between freezing wall circle closure time and flow velocity. By increasing flow velocity, the circle closure time of freezing wall increases non-linearly. With velocity greater than 1.5m/d, the closure time increases dramatically. **Figure 7** shows the variation curve between average wall thickness in each direction and corresponding flow velocity. The influence of flow velocity on the average thickness of the upstream wall is the most obvious.

5. Conclusions

Concluded with the results at different times, the temperature contour maps combined with permeability coefficient and groundwater flow velocity field (**Figure 5**) indicate that the freezing wall appears in an asymmetrical shape as the horizontal groundwater flow is normal to the axial of the tunnel. Along the groundwater flow direction, freezing wall forms slowly and on the upstream side the thickness of the freezing wall is thinner than that on the downstream side. The closure time of the freezing wall increases at the middle of the both up and downstream sides. The average thickness of the freezing wall on the upstream side is mostly affected by the groundwater flow velocity. With the successful validation of this model, this numerical simulation could provide further guidance in this AGF project in the future.

6. References

1. Harlan RL. Analysis of coupled heat-fluid transport in partially frozen soil. Water Resources Research 9 1314-23 (1973).
2. Jeffrey M. McKenzie, et. al. Groundwater flow with energy transport and water–ice phase change: Numerical simulations, benchmarks, and application to freezing in peat bogs. Advances in Water Resources 30 966-983 (2007).

3. Vitel M, Rouabhi A, Tijani M, et al. Modeling heat transfer between a freeze pipe and the surrounding ground during artificial ground freezing activities. Computers and Geotechnics 63 99-111 (2015).

4. Vitel M, Rouabhi A, Tijani M, et al. Modeling heat and mass transfer during ground freezing subjected to high seepage velocities. Computers and Geotechnics 73 1-15 (2016).

5. S. Papakonstantinou, G. Anagnostou, E. Pimentel. Evaluation of ground freezing data from the Naples subway. Ice (Geotechnical Engineering) 166 280-298 (2013).

6. Pimentel E, Papakonstantinou S, Anagnostou G. Numerical interpretation of temperature distributions from three ground freezing applications in urban tunnelling. Tunnelling and Underground Space Technology28 57-69 (2012).

7. Appendix

Table 1: Base case model parameters

Parameter	Value
Density of soil ρ_s (kg/m³)	1800
Density of water ρ_w (kg/m³)	1000
Density of ice ρ_i (kg/m³)	920
Thermal conductivity of soil λ_s (W/(m · K))	0.85
Thermal conductivity of water λ_w (W/(m · K))	0.6
Thermal conductivity of ice λ_i (W/(m · K))	2.14
Heat capacity of soil C_s (J/(kg · K))	1220
Heat capacity of water C_w (J/(kg · K))	4200
Heat capacity of ice C_i (J/(kg · K))	2100
Porosity n	0.4
Permeability coefficient k (m/d)	5
Latent heart of formation L (J/kg)	334720